

Article

# Wear Behavior of Mechanically Alloyed Ti-Based Bulk Metallic Glass Composites Containing Carbon Nanotubes

Yung-Sheng Lin <sup>1</sup>, Chih-Feng Hsu <sup>2</sup>, Jyun-Yu Chen <sup>3</sup>, Yeh-Ming Cheng <sup>3</sup> and Pee-Yew Lee <sup>3,\*</sup>

<sup>1</sup> Department of Chemical Engineering, National United University, Miaoli 360, Taiwan; linsy@nuu.edu.tw

<sup>2</sup> Chenming Mold Ind. Corp., Taipei 114, Taiwan; William\_Hsu@tw.uneec.com

<sup>3</sup> Institute of Materials Engineering, National Taiwan Ocean University, Keelung 202, Taiwan; 10455016@ntou.edu.tw (J.-Y.C.); zzz200583815@gmail.com (Y.-M.C.)

\* Correspondence: pylee@ntou.edu.tw; Tel.: +886-2-2469-3078; Fax: +886-2-2462-5324

Academic Editor: Chun-Liang Chen

Received: 23 August 2016; Accepted: 11 November 2016; Published: 21 November 2016

**Abstract:** The present paper reports the preparation and wear behavior of mechanically alloyed Ti-based bulk metallic glass composites containing carbon nanotube (CNT) particles. The differential scanning calorimeter results show that the thermal stability of the amorphous matrix is affected by the presence of CNT particles. Changes in glass transition temperature ( $T_g$ ) and crystallization temperature ( $T_x$ ) suggest that deviations in the chemical composition of the amorphous matrix occurred because of a partial dissolution of the CNT species into the amorphous phase. Although the hardness of CNT/Ti<sub>50</sub>Cu<sub>28</sub>Ni<sub>15</sub>Sn<sub>7</sub> bulk metallic glass composites is increased with the addition of CNT particles, the wear resistance of such composites is not directly proportional to their hardness, and does not follow the standard wear law. A worn surface under a high applied load shows that the 12 vol. % CNT/Ti<sub>50</sub>Cu<sub>28</sub>Ni<sub>15</sub>Sn<sub>7</sub> bulk metallic glass composite suffers severe wear compared with monolithic Ti<sub>50</sub>Cu<sub>28</sub>Ni<sub>15</sub>Sn<sub>7</sub> bulk metallic glass.

**Keywords:** mechanical alloying; bulk metallic glass composite; super-cooled liquid region; vacuum hot pressing; wear

## 1. Introduction

Ever since the first bulk metallic glasses (BMGs) were synthesized in 1989 [1], considerable progress has been made in the preparation of BMGs. A great number of multicomponent metallic glass alloys with strong glass-forming ability and high thermal stability have been discovered, such as Ti, Zr, Fe, Pd, Mg, Cu, Ni, and other metallic glass alloy systems [2–4]. BMGs have attracted much attention because of their unique properties, such as their remarkable levels of strength, hardness, corrosion resistance, and wear resistance. However, BMGs usually exhibit little overall room temperature plasticity because of the formation of highly localized shear banding, which may result in catastrophic failures [5]. Attempts have been made to enhance the ductility of BMGs by reducing their dimensions, thereby mitigating the catastrophic effects of instabilities on the material behavior [6]. A decrease in the aspect ratio of the sample (i.e., samples with small dimensions in the directions perpendicular to the applied load) generates an interaction in the form of deflected shear bands with a wavy shape [7]. Jiang et al. [8] conducted compression tests on specimens with different height ( $h$ ) to diameter ( $d$ ) ( $h/d$ ) ratios for Zr<sub>52.5</sub>Cu<sub>17.9</sub>Ni<sub>14.6</sub>Al<sub>10</sub>Ti<sub>5</sub>. Plasticity reached almost 80% for the specimens with an  $h/d$  ratio of 0.5, which was much higher than the 2% plasticity of specimens with an  $h/d$  ratio of 2. The researchers attributed these differences to the effect of specimen geometry, in which the platen can hinder the excessive propagation of shear bands from the premature fracture. Metallic glass matrix composites have been developed to improve the mechanical properties of such single-phase metallic

glass alloys. Such glasses are ex situ, reinforced by second-phase particulates, fibers, or in situ formed ductile phase precipitates [9]. It was discovered that the existence of ceramic or insoluble metallic particles inside the glass matrix can suppress the propagation of shear bands, thereby increasing the toughness and ductility of the metallic glass matrix composite.

Ti-based BMGs were first reported in a Ti-Zr-Ni-Be system in 1994 [10]. Many techniques have been applied successfully to prepare Ti-based BMGs, but most research efforts and industrial inquiries have focused on different methods of implementation for rapid solidification [11]. An alternative method is using solid-state amorphization processing such as mechanical alloying (MA) to prepare amorphous powders that are suitable for further compaction and densification. This method facilitates the introduction of reinforcing particles into the glassy matrix. As previous investigations have demonstrated, MA has been successfully applied for the preparation of amorphous Cu- and Zr-based composite powders [12,13]. Carbon nanotubes (CNTs) are endowed with exceptionally high material properties very close to their theoretical limits, such as electrical and thermal conductivity, strength, stiffness, and toughness. Therefore, CNTs are the latest reinforcement materials employed in composites, owing to their possessing structural properties stronger than those of any metal [14]. Kim et al. [15] reported that carbon fiber-reinforced BMG composites can be successfully prepared by infiltrating liquid Zr-Ti-Cu-Ni-Be into carbon fiber bundles. Shortly after this, Bian et al. [16–19] synthesized CNT-reinforced BMG composites, which exhibit excellent wave absorption properties.

The advantages of BMGs render them most suitable for application in small structural parts. For industrial applications, detailed information about wear performance is required, but only a few previous studies have reported on this. The first reported wear test was a pin-on-disk study of the abrasive wear of Pd-Si-Cu metallic glasses [20]. Gloriant classified Zr-based bulk glassy alloy in the hardened alloy group with regard to the relationship between its hardness and wear resistance [21]; however, despite increasing demand, few studies have been published on the mechanism of wear in bulk glassy alloys, and therefore numerous unique characteristics are yet to be defined.

Even though BMGs and CNTs possess many excellent properties, a literature survey indicated that no report exists on the formation of a Ti-based BMG composite powder containing CNT particles using the MA process. For the present study, amorphous  $\text{Ti}_{50}\text{Cu}_{28}\text{Ni}_{15}\text{Sn}_7$  powders both with and without the addition of CNT particles were prepared using MA. Subsequent consolidation of as-milled powders was performed, and the mechanical properties of the compacts were evaluated by Vickers microhardness and wear property testing.

## 2. Experimental

Elemental powders of Ti (99.7%, <325 mesh), Cu (99.9%, <325 mesh), Ni (99.9%, <300 mesh), Sn (99.999%, 100 mesh), and CNTs (99.999%, <325 mesh) were weighed to yield the desired  $\text{Ti}_{50}\text{Cu}_{28}\text{Ni}_{15}\text{Sn}_7$  or CNT/ $\text{Ti}_{50}\text{Cu}_{28}\text{Ni}_{15}\text{Sn}_7$  composition. The mixture of elemental metallic powders with the nominal composition of  $\text{Ti}_{50}\text{Cu}_{28}\text{Ni}_{15}\text{Sn}_7$  (in at. %) was mechanically alloyed with or without the addition of 4, 8, and 12 vol. % CNT powders. Milling was performed in a SPEX 8016 shaker ball mill (SPEX SamplePrep, Metuchen, NJ, USA) under an Ar atmosphere. Specific details of the MA process are described elsewhere [12]. The as-milled composite powders were consolidated in a vacuum hot pressing machine to prepare bulk samples, each of which had a 10 mm diameter and a 2 mm thickness. Hot pressing was performed at 723 K under a pressure of  $-1.20$  GPa and a high-vacuum (approximately  $10^{-3}$  Torr) environment.

The structures of both the as-milled powders and bulk samples were analyzed using a Siemens D 5000 X-ray diffractometer (Siemens AG, Karlsruhe, Germany) and a Hitachi-4100 scanning electron microscope (SEM) (Hitachi High-Technologies Corporation, Tokyo, Japan). Thermal analysis was investigated using a Dupont 2000 differential scanning calorimeter (DSC) (TA instruments, New Castle, PA, USA), in which the sample was heated from room temperature to 900 K under a purified Ar atmosphere at a constant heating rate of 40 K/min. In addition, the Vickers microhardness tests of consolidated BMG specimens were measured with a Matsuzawa MXT50-UL machine (Matsuzawa Co.,

Ltd., Akita-shi, Japan) using a static load of 0.5 N. The friction and wear behaviors of  $\text{Ti}_{50}\text{Cu}_{28}\text{Ni}_{15}\text{Sn}_7$  composite specimens both with and without CNT particles were tested under unlubricated conditions on a block-on-roller TE53 wear tester from Plint Co., Kingsclere, UK. The roller material was hardened and tempered AISI O1 tool steel in 65 HRC (832 HV in microhardness). The wear test was performed under selected contact pressures of 5, 10, 15, and 20 N at a revolution speed of 200 rpm. The weight loss of the specimen was recorded using an OHAUS AP250D-0 electronic balance (OHAUS Co., Parsippany, NJ, USA). Samples of JIS SKH-2 high-speed tool steel with a hardness of 24 and  $\text{Ti}_{50}\text{Cu}_{28}\text{Ni}_{15}\text{Sn}_7$  crystalline alloy with a hardness of 29 were also tested for comparative purposes.

### 3. Results and Discussion

Figure 1 shows the X-ray diffraction (XRD) patterns of  $\text{Ti}_{50}\text{Cu}_{28}\text{Ni}_{15}\text{Sn}_7$  after the addition of 4–12 vol. % CNT particles after 8 h of milling. For the plain  $\text{Ti}_{50}\text{Cu}_{28}\text{Ni}_{15}\text{Sn}_7$  alloy and the matrix with 4 vol. % CNT particles, only a broad diffraction peak appears around  $2\theta = 42^\circ$ , indicating the formation of fully amorphous powders. This may be attributed to the small volume fraction of CNT particles and their small crystalline size. The findings of the present study are similar to the observations regarding the preparation of the  $\text{Al}_2\text{O}_3/\text{NiAl}$  intermetallic-matrix composite reported by Lin et al. [22], in that, for small  $\text{Al}_2\text{O}_3$  additions in mechanically alloyed Ni-Al alloys, no  $\text{Al}_2\text{O}_3$  phase was detected by XRD after 10 h of milling. In the case of 12 vol. % CNT powders, crystalline TiC diffraction peaks were observed superimposed on the amorphous broad diffraction peaks. Similar behavior was reported by Sun et al. [23], who examined  $\text{Cu}_{47}\text{Ti}_{34}\text{Zr}_{11}\text{Ni}_8$  with graphite flakes. It is well known that metalloidal carbon can form strong covalent bonds with metallic constituents, causing the subsequent formation of easily nucleated crystalline compounds [24,25]. The activation energy of TiC formation was calculated as 731.6 kJ/mol [26].

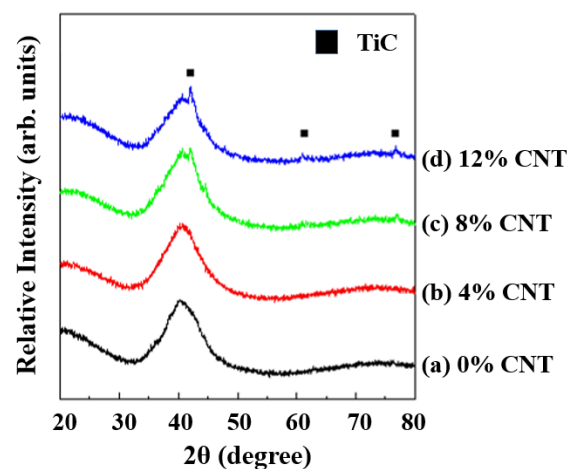


**Figure 1.** X-ray diffraction (XRD) patterns for mechanically alloyed  $\text{Ti}_{50}\text{Cu}_{28}\text{Ni}_{15}\text{Sn}_7$  and composite powders after 8 h milling: (a) 0% carbon nanotube (CNT); (b) 4% CNT; (c) 8% CNT; (d) 12% CNT.

Differential scanning calorimetry was applied to investigate the glass transition and crystallization behavior of the as-milled powders. The DSC scans of the 8 h as-milled  $\text{Ti}_{50}\text{Cu}_{28}\text{Ni}_{15}\text{Sn}_7$  monolithic glass and the composites with CNT particles are presented in Figure 2. The glass transition ( $T_g$ ) and crystallization ( $T_x$ ) temperatures were defined as the onset temperature of the endothermic and exothermic DSC events, respectively. The  $T_g$  and  $T_x$  were 719 and 765 K, respectively, for the  $\text{Ti}_{50}\text{Cu}_{28}\text{Ni}_{15}\text{Sn}_7$  without CNT particles. The glass transition temperature ( $T_g$ ) and the crystallization temperature ( $T_x$ ) of the composite powders were higher than those of single-phase amorphous  $\text{Ti}_{50}\text{Cu}_{28}\text{Ni}_{15}\text{Sn}_7$  alloys. The addition of CNT particles into the glassy matrix induced a shift to higher temperatures for both  $T_g$  and  $T_x$ . This suggests that a small amount of CNT particles might be alloyed into the matrix upon milling, thereby changing the overall composition of the glassy phase.

Similar behavior was reported for small ZrC additions by MA in a Zr-Al-Cu-Ni alloy [27]; hence, slight deviations must be taken into account when explaining changes in the thermal stability of the composite powders. According to the heat of thermodynamic mixing ( $\Delta H$ ) [28], the heat of mixing in Ti and C is  $-151$  kJ/mol, which is the highest of all the elements in the present study (Ti, Cu, Ni, Sn, and CNT). It was observed that Ti and a metalloid carbon with strong covalent bonds could be synthesized as TiC, thereby changing the matrix component in the composite materials.

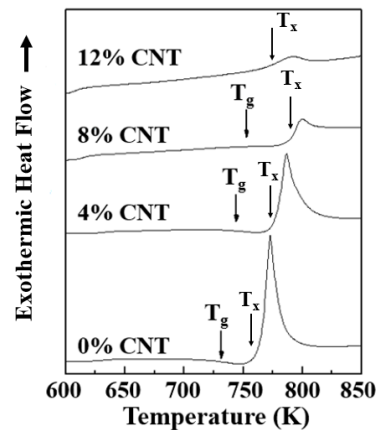


**Figure 2.** Differential scanning calorimeter (DSC) scans of mechanically alloyed  $\text{Ti}_{50}\text{Cu}_{28}\text{Ni}_{15}\text{Sn}_7$  and composite powders after 8 h milling.  $T_g$ : Glass transition temperature;  $T_x$ : Crystallization temperature.

Transmission electron microscopy (TEM) bright field images and diffraction patterns were analyzed to examine the amorphization and the nanocrystallization of  $\text{Ti}_{50}\text{Cu}_{28}\text{Ni}_{15}\text{Sn}_7$  monolithic glass and composites with 12% vol. CNT particles. The TEM images of amorphous  $\text{Ti}_{50}\text{Cu}_{28}\text{Ni}_{15}\text{Sn}_7$  and the composite powders are shown in Figure 3. In the TEM micrographs of  $\text{Ti}_{50}\text{Cu}_{28}\text{Ni}_{15}\text{Sn}_7$  powder, a typical “salt and pepper” microstructure representing a homogeneous amorphous phase can be noticed. TEM micrographs of the composite with 12% vol. CNT particles and a crystalline TiC diffraction pattern can be observed. The diffraction pattern displayed a diffuse halo beside the ring pattern of crystalline TiC, indicating the formation of an amorphous phase that coexisted with the TiC particles. Numerous TiC particles of irregular shapes and sizes, with diameters ranging from 20 to 40 nm, were embedded and homogeneously distributed in the matrix of the amorphous Ti-based alloy.

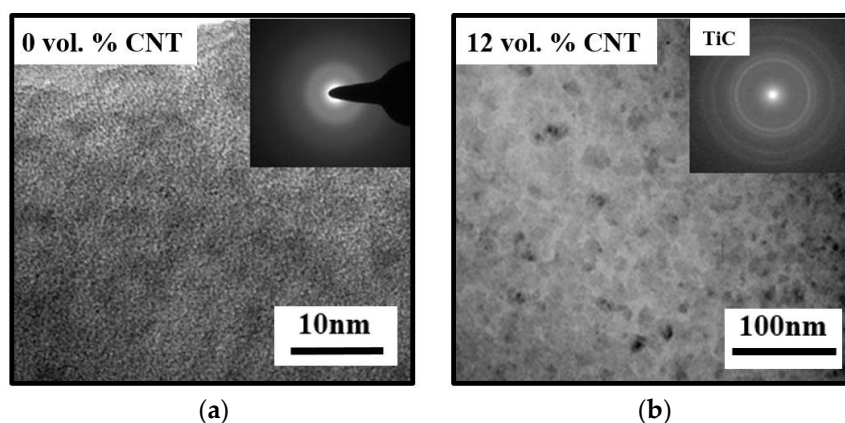


**Figure 3.** Transmission electron microscopy (TEM) images of mechanically alloyed  $\text{Ti}_{50}\text{Cu}_{28}\text{Ni}_{15}\text{Sn}_7$  and composite powders after 8 h milling: (a) 0% CNT; (b) 12% CNT.

Based on the DSC results, the 8 h as-milled composite powders were consolidated into a disk through vacuum hot pressing with a 10 mm diameter and a 2 mm thickness. The powders were hot pressed at 723 K under a pressure of 1.2 GPa for 30 min. Figure 4 shows a consolidated sample of a bulk metallic glass composite; it exhibited a smooth outer surface and a metallic luster. XRD and DSC analyses were performed to confirm the amorphization status of the consolidated samples. Though not shown here, consolidated BMG  $\text{Ti}_{50}\text{Cu}_{28}\text{Ni}_{15}\text{Sn}_7$  and the composite samples exhibited similar XRD and DSC results as those of the corresponding powders shown in Figure 1 (XRD) and Figure 2 (DSC).

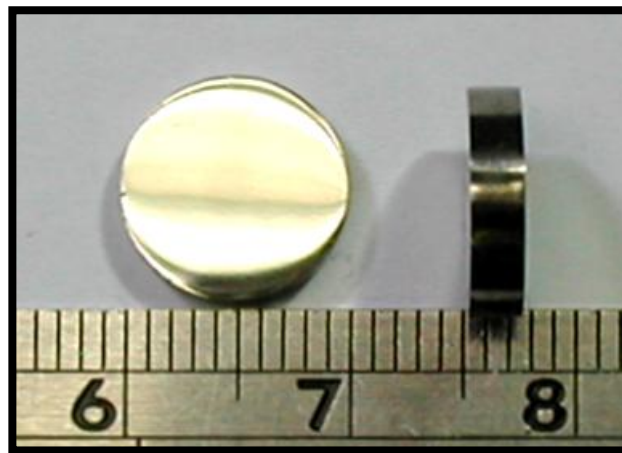


**Figure 4.** Outer morphology of  $\text{Ti}_{50}\text{Cu}_{28}\text{Ni}_{15}\text{Sn}_7$  with 4% vol. CNT particles after vacuum hot pressing at 723 K under a pressure of 1.2 GPa.

The cross-sectional view of the consolidated  $\text{Ti}_{50}\text{Cu}_{28}\text{Ni}_{15}\text{Sn}_7$  BMG and composite samples examined by SEM is shown in Figure 5. No significant pores were observed in the cross-sectional view taken at magnification of 20,000 times, which reveals that relatively dense  $\text{Ti}_{50}\text{Cu}_{28}\text{Ni}_{15}\text{Sn}_7$  bulk composite samples can be successfully fabricated by using vacuum hot pressing. Meanwhile, the CNT particle is hard to observe in the SEM image. The main reason for this is probably due to its nanometer size. The density value of the monolithic  $\text{Ti}_{50}\text{Cu}_{28}\text{Ni}_{15}\text{Sn}_7$  bulk sample as measured by the Archimedes method was  $6.51 \text{ g/cm}^3$ , while those for the composite samples containing 4%, 8%, and 12% vol. CNT particles were  $6.44$ ,  $6.43$  and  $6.37 \text{ g/cm}^3$ , respectively, leading to a relative density value of 97.8%, 94.7%, 94.4%, and 94.0%, correspondingly.

Figure 6 shows the mechanical properties of BMG composite samples evaluated using Vickers microhardness testing. Because a relatively high density was achieved, the influence of porosity on the  $\text{Ti}_{50}\text{Cu}_{28}\text{Ni}_{15}\text{Sn}_7$  BMG and its composites in the present study can be neglected. The Vickers microhardness for the  $\text{Ti}_{50}\text{Cu}_{28}\text{Ni}_{15}\text{Sn}_7$  BMG disc was 6.85 GPa, which was higher than the values of the Ti-based amorphous ribbons (which ranged from 6.02 to 6.56 GPa) prepared by melt spinning [2], mechanically alloyed  $\text{Zr}_{55}\text{Al}_{10}\text{Cu}_{30}\text{Ni}_{5}$  BMG composites (5.6 to 6.1 GPa), and  $\text{Zr}_{65}\text{Al}_{7.5}\text{Cu}_{17.5}\text{Ni}_{10}$  composites (4.9 to 5.7 GPa) [29]. The microhardness of the  $\text{Ti}_{50}\text{Cu}_{28}\text{Ni}_{15}\text{Sn}_7$  BMG composites with 12% vol. CNT particles was 9.34 GPa. No cracks were observed around the indentation either from the corners or sides, which implies that the BMG composites are sufficiently tough to prevent fractures. The microhardness readings of the specimens of SKH-2 high-speed steel and crystalline  $\text{Ti}_{50}\text{Cu}_{28}\text{Ni}_{15}\text{Sn}_7$  alloy were 5.41 and 6.69 GPa, respectively. The difference in microhardness may be attributed to the in situ formed TiC particles and residual stress generated as a result of the differences in the coefficients of thermal expansion between the amorphous matrices and the TiC particulates, resulting in a high density of dislocations [30,31].

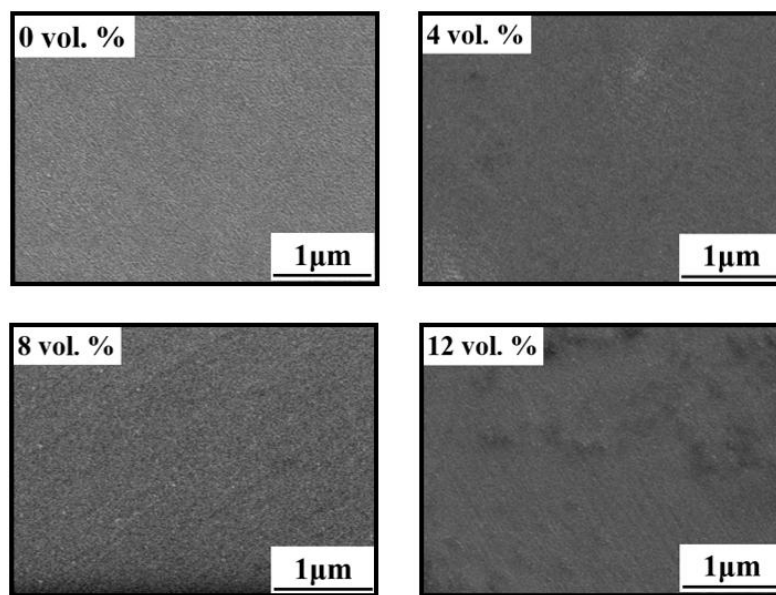


**Figure 5.** Cross-sectional scanning electron microscope (SEM) image of the  $\text{Ti}_{50}\text{Cu}_{28}\text{Ni}_{15}\text{Sn}_7$  bulk metallic glasses (BMG) and composite samples after vacuum hot pressing at 723 K under a pressure of 1.2 GPa.

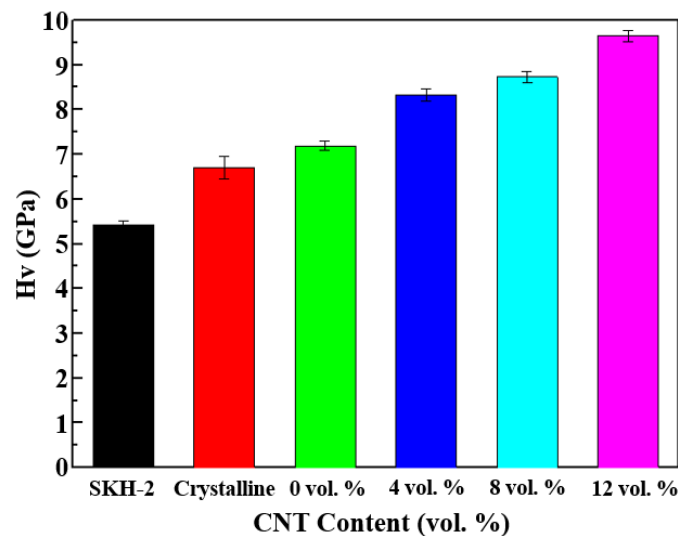


**Figure 6.** Microhardness of SKH-2 steel, crystalline Ti-based alloy, and CNT/ $\text{Ti}_{50}\text{Cu}_{28}\text{Ni}_{15}\text{Sn}_7$  BMG composite specimens. Hv: The Vickers hardness number.

Samples of the Ti-based BMG composite, crystalline Ti-based alloy and SKH-2 specimen were tested for wear resistance and friction on a block-on-roller wear tester under unlubricated conditions. Quenched and tempered JIS SKS3 (AISI O1) tool steel with 65 HRC (832 HV) was selected as the roll material. Contact pressures of 5, 10, 15, and 20 N were exerted on the tops of the specimens for the wear test, and the roller rotation speed was set to 200 rpm. The steady-state friction coefficients for the six different specimens tested on block-on-roller devices are illustrated in Figure 7. Under these wear configurations, the coefficients of friction (COFs) of the Ti-based BMG composites and conventional materials were measured within the range 0.45–0.85; their values within the range depended on the normal load and the test environment. In a comparison of the steady-state COFs of various specimens, the COFs of SKH-2 and crystalline Ti-based alloy were higher than those of the Ti-based

BMG composites; furthermore, the COFs decreased as the applied load increased [21,32]. It is notable that COFs of the  $\text{Ti}_{50}\text{Cu}_{28}\text{Ni}_{15}\text{Sn}_7$  BMG matrix can be reduced with the addition of CNT particles. In contrast to frictional behavior, the results of the present study indicate noteworthy differences in performance; under a high load (20 N), the BMG composites containing 12% vol. CNT particles exhibited the highest COFs, whereas the wear performance levels of the monolithic Ti-based BMG and the matrices with 4–8 vol. % CNT particles were higher than those of the matrix with 12 vol. % CNT particles. The soft SKH-2 was found to possess lower wear resistance, whereas the hard Ti-based BMG composites containing 12 vol. % CNT particles did not exhibit the highest wear performance levels. Similar results were also found in various BMG systems of different microhardness levels; Fleury et al. [32] reported that Ni-based BMGs exhibit higher microhardness levels than Ti- or Zr-based BMGs do, but also that wear resistance levels of Ni-based BMGs are not as high as those of Ti- or Zr-based BMGs.

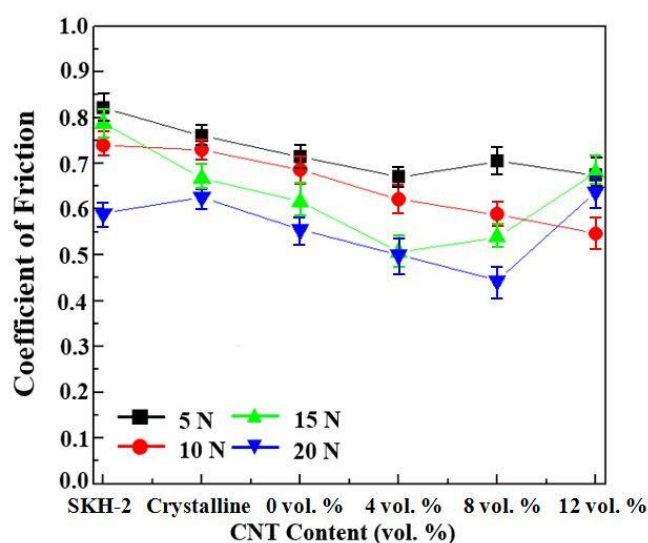


**Figure 7.** Effects of CNT volume fraction on the friction coefficients of  $\text{Ti}_{50}\text{Cu}_{28}\text{Ni}_{15}\text{Sn}_7$  BMG composites under different loads.

Figure 8 illustrates the cumulative wear mass losses of various specimens tested under the contact pressure of different applied loads on the block-on-roller wear tester. The wear mass losses of the Ti-based BMGs with both 4 and 8 vol. % CNT particles were lower than those of SKH-2 and crystalline Ti-based alloy specimens; however, the wear mass loss of hardness in the matrix with 12 vol. % particles was higher than that of the other Ti-based BMG composites. We can conjecture that the hardness level of the matrix with 12 vol. % CNT particles is higher than that of the roller (8.23 GPa), and that the friction wear force of the roller repeatedly wears on the matrix with 12 vol. % CNT particles, thereby altering the wear configuration. The wear behavior of the matrix with 12 vol. % CNT particles was transferred to the roller for reinforcement. The reinforced matrix with 12 vol. % CNT particles peeled easily as a result of wear from the roller, subsequently causing debris, and the peeled debris became attached to the roller. When the roller motion was repeated, the wear behavior was transferred to the debris of the matrix with 12 vol. % CNT particles, thereby inducing an increase in both COFs and the wear behavior.

Concerning the mechanisms of abrasive wear in Ti-based BMG composites, Figure 9 shows the surface tracks for the monolithic Ti-based BMG, the matrix with 12 vol. % CNT composites, the crystalline Ti-based alloy, and the SKH-2 specimen after tests were performed under different applied loads. It can be observed from the micrographs of SKH-2 that a ditch-like microstructure formed on the surface along the sliding direction. This wear mechanism possesses the characteristics of typical adhesive wear. Adhesive wear occurs when the contact pressure between rolling surfaces is high

enough to cause local plastic deformation and welding between the contacting asperities [33], whereas the crystalline Ti-based alloy exhibited less adhesive wear on the surface. The Ti-based BMG and the matrix with 12 vol. % CNTs exhibited an abrasive wear track. Abrasive wear occurs when hard debris particles are indented and form a groove on the rolling surface of the material [33]. Energy-dispersive X-ray spectroscopy (EDS) analysis of the wear tracks indicated that the dark areas of the JIS SKS3 tool steel were rich in Fe, suggesting that material transfer occurred from the soft counterpart rolling to the hard Ti-based BMG composites. Similar behavior has been reported by Fleury et al. and Liu et al. [32,34], regarding examinations of different BMG systems and  $\text{Si}_3\text{N}_4$ -based composites. Kalin et al. [35] reported that the model for wear behavior should include chemical reactions, spot temperatures, thermal conductivity, and phase transformations.

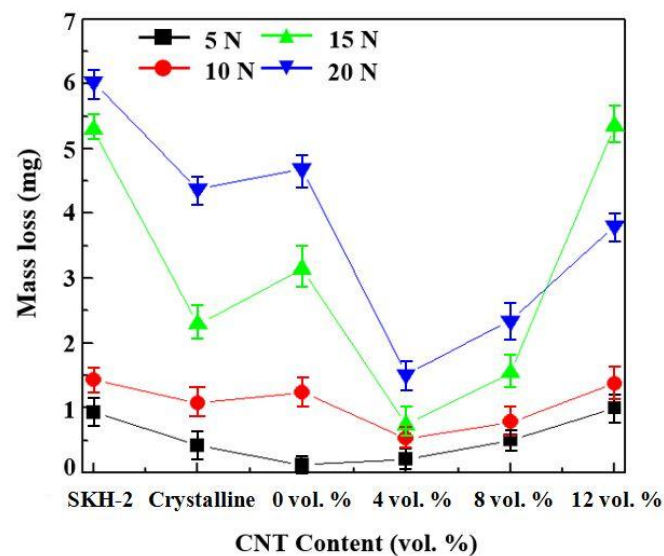


Figure 8. Mass loss of CNT/Ti<sub>50</sub>Cu<sub>28</sub>Ni<sub>15</sub>Sn<sub>7</sub> bulk metallic glass composites under different loads.

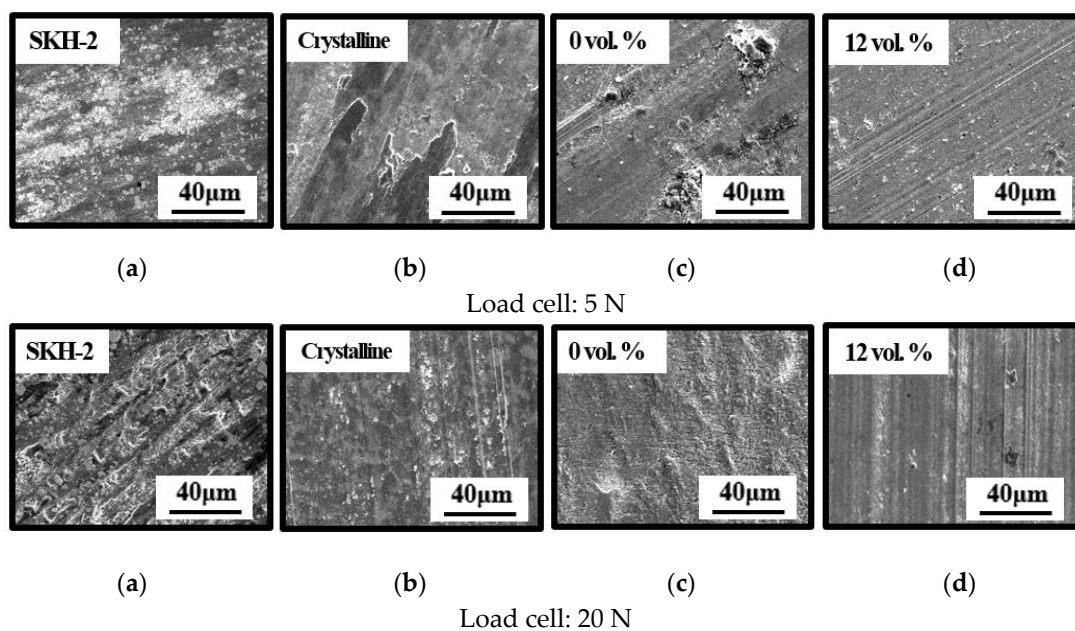


Figure 9. SEM micrographs of the worn surfaces of SKH-2 steel, crystalline Ti-based alloy, and CNT/Ti<sub>50</sub>Cu<sub>28</sub>Ni<sub>15</sub>Sn<sub>7</sub> BMG composite specimens: (a) SKH-2 steel; (b) crystalline Ti-based alloy; (c) 0% CNT; (d) 12% CNT.

#### 4. Conclusions

In the present study, amorphous  $\text{Ti}_{50}\text{Cu}_{28}\text{Ni}_{15}\text{Sn}_7$  and its composite powders were successfully synthesized through an MA process performed on powder mixtures of pure Ti, Cu, Ni, Sn, and CNT after 8 h milling. The metallic glass composite powders exhibited a large supercooled liquid region before crystallization. The thermal stability of the amorphous matrix was affected by the presence of CNT particles. Changes in  $T_g$  and  $T_x$  suggest that deviations in the chemical composition of the amorphous matrix occurred because of a partial dissolution of the CNT species in the amorphous phase. BMG composite discs were obtained by consolidating the 8 h as-milled composite powders through a vacuum hot pressing process. The Vickers microhardness test results were 6.85 GPa for the  $\text{Ti}_{50}\text{Cu}_{28}\text{Ni}_{15}\text{Sn}_7$  BMG, and 7.96, 8.42, and 9.34 GPa for the composites containing 4%, 8%, and 12% vol. CNT particles, respectively. Notable levels of hardness (approximately 30%) were achieved for the  $\text{Ti}_{50}\text{Cu}_{28}\text{Ni}_{15}\text{Sn}_7$  BMG composites comprising 12 vol. % CNT particles; however, the wear mass loss of the Ti-based BMG composite with 12 vol. % CNT particles (the composite with the highest hardness) was higher than that of the other Ti-based BMG composites containing 4 and 8 vol. % CNT particles when tested under different applied loads. The results demonstrate that the wear resistance levels of Ti-based BMG composites do not correlate with their hardness levels because they do not follow the wear law. Wear surfaces under high applied loads demonstrate that the matrix with 12 vol. % CNT particles suffered severe wear compared with the monolithic Ti-based BMG.

**Acknowledgments:** The authors are grateful for the financial support of this study by the Ministry of Science and Technology of the Taiwan under Grant No. MOST 103-2221-E-019-013.

**Author Contributions:** Yung-Sheng Lin and Chih-Feng Hsu carried out the sample preparation and data analysis work. Jyun-Yu Chen conducted the SEM study. The measurement of wear properties was performed by Yeh-Ming Cheng. Pee-Yew Lee designed the experimental procedure and prepared the manuscript of the paper.

**Conflicts of Interest:** The authors declare no conflict of interest.

#### References

- Inoue, A.; Zhang, T.; Masumoto, T. Al-La-Ni Amorphous Alloys with a Wide Supercooled Liquid Region. *Mater. Trans. JIM* **1989**, *30*, 965. [[CrossRef](#)]
- Zhang, T.; Inoue, A. Thermal and Mechanical Properties of Ti-Ni-Sn Amorphous Alloys with a Wide Supercooled Liquid Region before Crystallization. *Mater. Trans. JIM* **1998**, *39*, 1001. [[CrossRef](#)]
- Yim, H.C.; Xu, D.H.; Johnson, W.L. Ni-based bulk metallic glass formation in the Ni-Nb-Sn and Ni-Nb-Sn-X (X = B, Fe, Cu) alloy systems. *Appl. Phys. Lett.* **2003**, *82*, 1030.
- Zhang, T.; Inoue, A. New Bulk Glassy Ni-based Alloys with High Strength of 3000MPa. *Trans. JIM* **2002**, *43*, 708.
- Hofmann, D.C. Shape memory bulk metallic glass composites. *Science* **2010**, *329*, 1294. [[CrossRef](#)] [[PubMed](#)]
- Ghidelli, M.; Gravier, S.; Blandin, J.-J.; Djemia, P.; Momprou, F.; Abadias, G.; Raskinb, J.-P.; Pardo, T. Extrinsic mechanical size effects in thin ZrNi metallic glass films. *Acta Mater.* **2015**, *90*, 232. [[CrossRef](#)]
- Greer, J.R.; de Hosson, J.T.M. Plasticity in small-sized metallic systems: Intrinsic versus extrinsic size effect. *Prog. Mater. Sci.* **2011**, *56*, 654. [[CrossRef](#)]
- Jiang, W.H.; Fan, G.J.; Choo, H.; Liaw, P.K. Ductility of a Zr-based bulk-metallic glass with different specimen's geometries. *Mater. Lett.* **2006**, *60*, 3537. [[CrossRef](#)]
- Schuh, C.A.; Hufnagel, T.C.; Ramamurty, U. Mechanical behavior of amorphous alloys. *Acta Mater.* **2007**, *55*, 4067. [[CrossRef](#)]
- Peker, A.; Johnson, W.L. Beryllium Bearing Amorphous Metallic Alloys Formed by Low Cooling Rates. U.S. Patent 5,288,344, 22 February 1994.
- Inoue, A. Synthesis and Properties of Ti-Based Bulk Amorphous Alloys with a Large Supercooled Liquid Region. *Mater. Sci. Forum* **1999**, *312–314*, 307.
- Wang, C.C.; Lin, C.K.; Lin, Y.L.; Chen, J.S.; Jen, R.R.; Lee, P.Y. Cu-Zr-Ti Bulk Metallic Glass Composites Produced by Mechanical Alloying and Vacuum Hot-Pressing. *Mater. Sci. Forum* **2005**, *475–479*, 3443. [[CrossRef](#)]

13. Eckert, J.; Seidel, M.; Kubler, A.; Klement, U.; Schultz, L. Oxid Dispersion Strengthened Mechanically Alloyed Amorphous Zr-Al-Cu-Ni Composites. *Scr. Mater.* **1998**, *38*, 595. [[CrossRef](#)]
14. Sinnott, S.B.; Andrews, R. Carbon Nanotubes: Synthesis, Properties, and Applications. *Science* **2000**, *289*, 1730. [[CrossRef](#)]
15. Kim, C.P.; Bush, R.; Masuhr, A.; Yim, H.C.; Johnson, W.L. Processing of carbon-fiber-reinforced  $Zr_{41.2}Ti_{13.8}Cu_{12.5}Ni_{10.0}Be_{22.5}$  bulk metallic glass composites. *Appl. Phys. Lett.* **1997**, *79*, 1456. [[CrossRef](#)]
16. Bian, Z.; Wang, R.J.; Zhao, D.Q. Excellent Ultrasonic Absorption Ability of Carbon-Nanotube-Reinforced Bulk Metallic Glass Composites. *Appl. Phys. Lett.* **2003**, *82*, 2790. [[CrossRef](#)]
17. Bian, Z.; Pan, M.X.; Zhang, Y. Carbon-nanotube-reinforced  $Zr_{52.5}Cu_{17.9}Ni_{14.6}Al_{10}Ti_5$  bulk metallic glass composites. *Appl. Phys. Lett.* **2002**, *81*, 4739. [[CrossRef](#)]
18. Bian, Z.; Wang, R.J.; Wang, W.H.; Zhang, T.; Inoue, A. Carbon-Nanotube-Reinforced Zr-Based Bulk Metallic Glass Composites and Their Properties. *Adv. Funct. Mater.* **2004**, *14*, 55. [[CrossRef](#)]
19. Bian, Z.; Wang, R.J.; Pan, M.X.; Zhao, D.Q.; Wang, W.H. Excellent Wave Absorption by Zirconium-Based Bulk Metallic Glass Composites Containing Carbon Nanotubes. *Adv. Mater.* **2003**, *15*, 616. [[CrossRef](#)]
20. Boswell, P.G. The wear resistance of a liquid quenched metallic glass. *J. Mater. Sci.* **1979**, *14*, 1505. [[CrossRef](#)]
21. Gloriant, T. Microhardness and abrasive wear resistance of metallic glass and nanostructured composite materials. *J. Non-Cryst. Solids* **2003**, *316*, 96. [[CrossRef](#)]
22. Lin, C.K.; Hong, S.S.; Lee, P.Y. Formation of NiAl- $Al_2O_3$  intermetallic-matrix composite powders by mechanical alloying technique. *Intermetallics* **2000**, *8*, 1043. [[CrossRef](#)]
23. Sun, Y.F.; Shek, C.H.; Guan, S.K.; Wei, B.C.; Geng, J.Y. Formation, thermal stability and deformation behavior of graphite-flakes reinforced Cu-based bulk metallic glass matrix composite. *Mater. Sci. Eng. A* **2006**, *435–436*, 132. [[CrossRef](#)]
24. Warriar, S.G.; Lin, R.Y. TiC growth in C fiber/Ti alloy composites during liquid infiltration. *Scr. Metall. Mater.* **1993**, *29*, 147. [[CrossRef](#)]
25. Zhang, E.L.; Zeng, S.Y.; Yang, B.; Li, Q.C.; Bo, Y.; Ma, M.Z. A study on the kinetic process of reaction synthesis of TiC: Part I. Experimental research and theoretical model. *Metall. Mater. Trans. A* **1999**, *30*, 1147. [[CrossRef](#)]
26. Swift, G.A.; Koc, R. Formation Studies of TiC from Carbon Coated  $TiO_2$ . *J. Mater. Sci.* **1999**, *34*, 3083. [[CrossRef](#)]
27. Deledda, S.; Eckert, J.; Schultz, L. Nanocrystalline CaO and ZrC as a Second Phase in Amorphous Zr-Cu-Al-Ni Matrix Composites. *Mater. Sci. Forum* **2001**, *360–362*, 85. [[CrossRef](#)]
28. De Boer, F.R.; Boom, R.; Mattens, W.C.M.; Miedema, A.R.; Niessen, A.K. *Cohesion in Metals: Transit. Metal Alloy*; Elsevier Scientific Pub. Co.: New York, NY, USA, 1988; Volume 723.
29. Eckert, J.; Reger-Leonhard, A.; Weiß, B.; Heilmaier, M.; Schultz, L. Bulk Nanostructured Multicomponent Alloys. *Adv. Eng. Mater.* **2001**, *3*, 41. [[CrossRef](#)]
30. Sheng, L.Y.; Yang, F.; Guo, J.T.; Xi, T.F.; Ye, H.Q. Investigation on NiAl-TiC- $Al_2O_3$  composite prepared by self-propagation high temperature synthesis with hot extrusion. *Compos. Part B Eng.* **2013**, *45*, 785. [[CrossRef](#)]
31. Zhao, H.L.; Qiu, F.; Jin, S.B.; Jiang, Q.C. Compression properties and work-hardening effect of the NiAl-matrix composite with  $TaB_2$  and TaB. *Intermetallics* **2012**, *27*, 1. [[CrossRef](#)]
32. Fleury, E.; Lee, S.M.; Ahn, H.S.; Kim, W.T.; Kim, D.H. Tribological properties of bulk metallic glassed. *Mater. Sci. Eng. A* **2004**, *375–377*, 276. [[CrossRef](#)]
33. Chiu, L.H.; Wu, C.H.; Chang, H. Wear behavior of nitrocarburized JIS SKD61 tool steel. *Wear* **2002**, *253*, 778. [[CrossRef](#)]
34. Liu, C.C.; Huang, J.L. Tribological characteristics of  $Si_3N_4$ -based composites in unlubricated sliding against steel ball. *Mater. Sci. Eng. A* **2004**, *384*, 299. [[CrossRef](#)]
35. Kalin, M.; Vizintin, J.; Novak, S.; Drazic, G. Wear mechanisms in oil-lubricated dry fretting of silicon nitride against bearing steel contacts. *Wear* **1997**, *210*, 27. [[CrossRef](#)]

